Texture evolution of cold rolled and reversion annealed metastable austenitic CrMnNi steels

A Weidner[1], K Fischer[1], C Segel[1], G Schreiber[2] and H Biermann[1]
[1] Institute of Materials Engineering, Technische Universität Bergakademie Freiberg, Freiberg, Germany
[2] Institute of Materials Science, Technische Universität Bergakademie Freiberg, Freiberg, Germany
E-mail: weidner@ww.tu-freiberg.de

Abstract. A thermo-mechanical process consisting of cold rolling and subsequent reversion annealing was applied to high-alloy metastable austenitic CrMnNi steels with different nickel contents. As a result of the reversion annealing ultrafine grained material with a grain size in the range between 500 nm up to 4 µm were obtained improving the strength behavior of the material. The evolution of the texture of both the cold rolled states and the reversion-annealed states was studied either by X-ray diffraction or by EBSD measurements. The nickel content has a significant influence on the austenite stability and consequently also on the amount of the martensitic phase transformation. However, the developed textures in both steel variants with different austenite stability revealed the same behavior. In both investigated steels the texture of the reverted austenite is a pronounced Bs-type texture as developed also for the deformed austenite

1. Introduction

Low carbon, metastable austenitic stainless steels (CrMnNi-steels) exhibit excellent mechanical properties like concurrently high strength and high ductility as well as a high capability of deformation energy absorption [e.g. 1] due to the TRIP (TRansformation Induced Plasticity) and TWIP (TWinning Induced Plasticity) effects. However, produced as cast steels the yield strength of this class of materials is quite low (about 200 MPa) caused mainly by the large grain size (up to 2 mm). A well established method for enhancing the yield strength of the material is the thermo-mechanical controlled processing (TMCP) mainly applied on wrought steels [e.g.2]. However, even cast CrMnNi steels can be treated by TMCP as shown elsewhere [3]. A cold rolling process up to 90 % of thickness reduction followed by a conventional heat treatment at 700°C and different holding times lead to ultra-fine grained (ufg) reverted austenite. Mean grain sizes varying between 500 nm and 4 µm revealed an increase in the yield strength of the material up to 1 GPa. Several authors studied the evolution of the deformation and transformation textures already mainly in TWIP steels [e.g. 4], but to minor extend also in TRIP steels [e.g. 5]. The deformation texture of the deformed austenite at high cold rolling (CR) degrees is of brass (Bs) type, which is typical for materials with low stacking fault energy (SFE). The Bs-type texture is mainly described by two texture components – (i) a strong Brass (Bs) component ({110}<112>) and a well developed Goss (G) component ({110}<001>). The martensitic phase transformation during the plastic deformation of TRIP steels leads to the development of a transformation texture of deformation-induced α'-martensite. This texture can be characterized by strong components with <110> || rolling direction (RD) and <111> || normal direction, respectively. It was shown

that the variant selection between the austenite and the α'-martensite is related to Kurdjumov-Sachs relationship [6].
The aim of the present paper is to have closer look on the texture evolution in the low carbon high-alloy, metastable austenitic CrMnNi steels. It is focused on the influence of the austenite stability on the evolution of deformation as well as transformation texture.

2. Experimental details

The investigated materials were two high-alloy CrMnNi steels (16 wt% Cr, 6 wt% Mn, , 1 wt% Si, 0.05 wt% N, 0.08 wt% C) with different content of nickel (3.7 wt% and 7.1 wt%, respectively) in cast conditions [7] after solution heat treatment (0.5 h at 1050°C, N2 gas quenching). The initial cast state was characterized by a mean grain size up to 2mm (see ref. [3]). Due to the chemical composition and the dendritic solidification segregations some amount of ferromagnetic δ-ferrite phase (2 % for steel with 7.1 % Ni and up to 10 % for the steel with 3.7 % Ni) is apparent in the microstructure. Stripes of the cast material were cold rolled up to CRs of 50 %, 70 % and 90 %, respectively. The reversion annealing was performed at different temperatures (650°C up to 800°C) and different holding times (1 sec, 2.5 min, 5 min, 10 min, 20 min and 120 min). Details on the cold rolling procedure and the heat treatment are given in [3]. The volume fractions of the *b.c.c.* phase (deformation-induced α'-martensite and δ-ferrite) of the cold rolled plates and the reversion annealed states were investigated by X-ray diffraction (XRD) phase analysis, ferritescope measurements and measurements using magnetic balance. The texture measurements were performed using XRD (cold rolled states) and electron backscatter diffraction (EBSD) (reversion annealed states).

3. Results and discussion

3.1.Volume fraction of deformation-induced a'-martensite

The evolution of the volume fraction of deformation-induced α'-martensite was determined using XRD, ferritescope and magnetic balance. The average values of all three methods are summarized in Tab. 1. In addition, Tab. 1 contains the martensite start temperature M_s calculated according to [8] and the SFE [9]. It becomes evident that with decreasing nickel content the austenite stability as well as the SFE is reduced, which results in a higher tendency of martensitic phase transformation during plastic deformation. This is well expressed by the higher volume fraction of the ferromagnetic phase in the steel with 3.7 % nickel. Whereas the steel with 7.1 % nickel has about 70 % of ferromagnetic phase after a CR of 90% the steel with 3.7 % nickel is nearly completely martensitic already at CR of 50%.

Table 1: Volume fraction of ferromagnetic phase for the as-cast state and different cold rolled states, M_s, SFE.

	as-cast	**50 % CR**	**70 % CR**	**90 % CR**	**M_s** [8] **[°C]**	**SFE** [9] **[mJ/m²]**
7.1 % Ni	2	45	48	70	-30	17.5 ± 1.4
3.7 % Ni	25	90	100	100	60	8.1 ± 0.9

However, it should be noted that the steel with 3.7. % nickel contains already in the as-cast state about 25 % of ferromagnetic phase, which is related to the above mentioned δ-ferrite (10 %) and 15 % martensite coming from the cooling process.

3.2.Texture of cold rolled austenite

According to the different level of martensitic phase transformation differences in the deformation textures of both steel variants were expected. However, for the steel with 3.7. % nickel the texture evolution of the deformed austenite could not be measured since the volume fraction of the retained austenite (10 %) was too small for XRD texture measurements. Therefore, Figure 1 shows only the texture of the deformed austenite of the steel with 7.1 % nickel at CR = 90 %. The deformation texture of the austenite is clearly a Bs-type texture with a dominant Bs-component and a weaker G component. There is no indication for other

components like Copper (C) {112}<111> or S-component {123}<624>, which would be typical for materials with higher SFE.

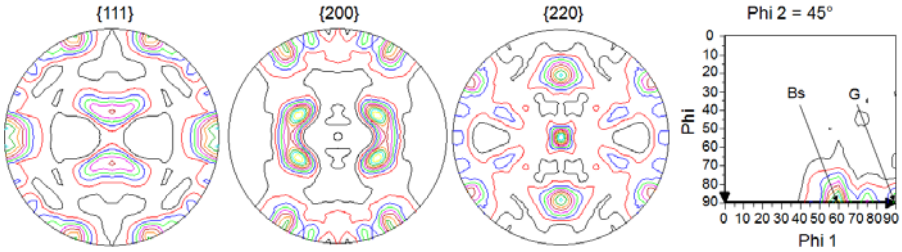

Figure 1: Texture of cold rolled austenite of the steel with 7.1 % nickel at cold rolling reduction of 90 %. {111}, {200} and {220} pole figures and the ODF section at constant Phi 2 = 45°.

3.3.Texture of deformation-induced α'-martensite

The texture evolution of the deformation-induced α'-martensite was followed for the steel with 3.7 % nickel for different CRs. Figure 2 illustrates the texture evolution using typical texture fibers known to develop in *b.c.c.* materials. At CR ≤ 70 % the formation of a strong {001}<110> component and a weaker {112}<110> component was observed. In addition, a well developed {111}<112> component is present, too. However, a significant change in the texture evolution occurred at CR > 70%. The {112}<110> component becomes more intense whereas the intensities of the other two components are decreased. A comparison with the texture in the steel with 7.1 % nickel at CR = 90% shows similar tendency. However, the texture components {112}<110> and {111}<112> are much more pronounced. Most probably, this related to the fact that in the steel with lower nickel content the martensitic phase transformation starts already at lower deformation degrees and no such strong Bs-type texture is developed during the lower CR levels.

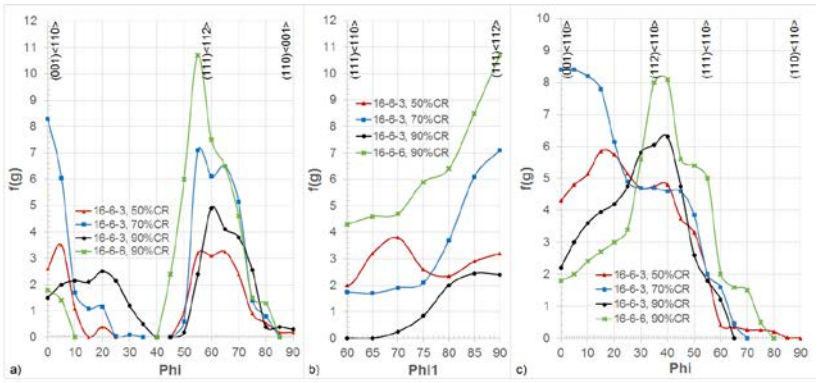

Figure 2: Texture evolution of the deformation-induced α'-martensite in the steel with 3.7 % nickel for CR of 50 %, 70 % and 90 %, respectively, in comparison to the steel with 7.1 % nickel at CR 90 %. (a) α-fiber (Phi1 = 0°, Phi2 = 45°). (b) γ-fiber (Phi2 = 45°, Phi = 55°). (c) ε-fiber (Phi 1 = 90°, Phi2 = 45°).

3.4.Textures of reverted states

Figure 3 shows the texture of the steel with 7.1 % nickel after CR = 90 % and different reversion annealing parameters. For all reversion annealing parameters a similar texture has developed, which is characterized by a pronounced Bs-component and a minor G-component as seen from the α-fiber shown in Fig. 3a. Thus, the transformation texture after the reversion annealing is comparable to the texture of the deformed austenite. However, as seen in Fig. 3b the τ-fiber reveals new components, which were not present in the cold rolled states. The main component along the τ-fiber is the C-component {112}<111> and its related components – the C_{twin} {552}<115> as well as the $C_{twin,\ rot}$ {332}<113>. However, it should be noted that about 30 % of deformed austenite remained in the microstructure at CR = 90 %. Therefore, there should be a similar amount of recrystallized and/or annealed austenite after the heat treatment. The components C, C_{twin} and $C_{twin,\ rot}$ are related according to [10] to the recrystallization process. However, the strong Bs-type texture after the reversion annealing can be taken according to

[10] as an indicator for a diffusionless shear transformation of the α'-martensite back into the austenite.

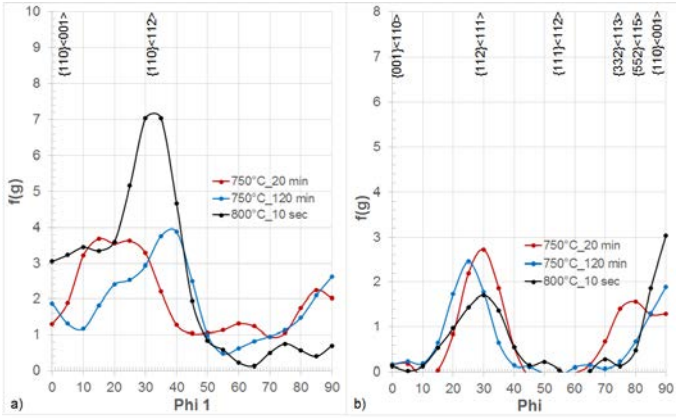

Figure 3: Texture evolution of the austenite in the steel with 7.1 % nickel at CR = 90% and different heat treatment parameters. (a) α-fiber (Phi = 45°, Phi2 = 0°). (b) τ-fiber (Phi1 = 90°, Phi2 = 45°).

The textures of the reverted states of the steel with 3.7 % nickel show similar behavior. However, in contrast to the steel with 7.1 % nickel recrystallized δ-ferrite is observed in the fully reverted austenitic microstructure.

4. Summary

The path of the texture transition in metastable CrMnNi steels during TMCP can be described by the following steps: (i) pronounced Bs-type texture with a strong Bs-component and weaker G-component, (ii) texture of α'-martensite with strong {112}<110> and {111}<112> components and a weaker {001}<110> component and (iii) pronounced Bs-type texture after reversion annealing again with strong Bs-component and weaker G-component. This transformation path is according to the literature related to the Kurdjumov-Sachs relations ship. In addition, the textures of the reverted states contain C, C_{twin} and $C_{twin,\ rot}$ components, which were not present in the cold rolled states. These components are related to the recrystallization process.

Acknowledgment

The authors acknowledge gratefully the German Research Foundation (DFG) for the financial support of the Collaborative Research Centre TRIP-Matrix-Composites (CRC 799). Furthermore, the authors thank Mr. U. Heinze (Institute of Metal Forming) and Dr.-Ing. T. Kreschel (Institute of Iron and Steel Technology) for the support performing the cold rolling and the heat treatment, respectively. Ms. K. Zuber is grateful acknowledge for the careful specimen preparation for EBSD measurements.

References

[1] S.Wolf, S. Martin, L. Krüger, U. Martin, *Mater. Sci. Eng. A* **594** (2014) 72–81.
[2] J. Mola, B.C. de Cooman, *Scripta Mater.* **65** (2011) 834–838.
[3] A. Weidner, A. Müller, A. Weiss, H. Biermann, *Mater. Sci. Eng. A* **573** (2013) 68–76.
[4] N.K. Tewary, S.K. Ghosh, S. Bera, D. Chakrabarti, S.Chatterjee, *Mater. Sci. Eng. A* **615** (2014) 400–415.
[5] S.G. Chowdhury, S. Datta, B.R. Kumar, P.K. Deb, R.N. Ghosh, *Mater. Sci. Eng. A* **443** (2007) 114–119.
[6] I.L. Dillamore and W.T. Roberts, *Acta Metall.*, **12**, (1964) 281–293.
[7] A. Weiß, H. Gutte, M. Radke, P.R. Scheller, *Patent specification* WO002008009722A1.
[8] A. Jahn, A. Kovalev, A. Weiss, P. R. Scheller, *Steel Res. Int.* **82** (2011) 1101–1108.
[9] D. Rafaja, C. Krbetschek, C. Ullrich, S. Martin, *J. Appl. Cryst.* **47** (2014) 936–946.
[10] B.R. Kumar, A.K. Singh, S. Das, D.K. Bhattacharya, *Mater. Sci. Eng. A* **364** (2004) 132–139.